Epileptiform activity in rat hippocampus strengthens excitatory synapses

Mathias H. Abegg, Natasa Savic, Markus U. Ehrengruber, R. Anne McKinney and Beat H. Gähwiler

Brain Research Institute, University of Zurich, Winterthurerstrasse 190, CH-8057 Zurich, Switzerland

Although epileptic seizures are characterized by excessive excitation, the role of excitatory synaptic transmission in the induction and expression of epilepsy remains unclear. Here, we show that epileptiform activity strengthens excitatory hippocampal synapses by increasing the number of functional (RS)-α-amino-3hydroxy-5methyl-4-isoxadepropionate (AMPA)-type glutamate receptors in CA3–CA1 synapses. This form of synaptic strengthening occludes long-term potentiation (LTP) and enhances long-term depression (LTD), processes involved in learning and memory. These changes in synaptic transmission and plasticity, which are fully blocked with *N*-methyl-D-aspartate (NMDA) receptor antagonists, may underlie epilepsy induction and seizure-associated memory deficits.

(Received 4 August 2003; accepted after revision 27 October 2003; first published online 31 October 2003)
Corresponding author M. H. Abegg: Brain Research Institute, University of Zurich, Winterthurerstrasse 190, CH-8057 Zurich, Switzerland. Email: mhabegg@access.unizh.ch

A variety of pathological (Commission on Classification and Terminology of the International League Against Epilepsy, 1989) and experimental conditions result in epilepsy, i.e. they are epileptogenic. A strong increase in neuronal activity such as a status epilepticus is a typical induction stimulus in experimental models of epilepsy: it can be achieved either pharmacologically (blockade of $GABA_A$ receptors (Traub *et al.* 1993), kainate application (Ben-Ari & Gho, 1988)) or by electrical stimulation (kindling; Goddard, 1967). Commonly the induction stimulus is followed by spontaneous recurrent seizures *in vivo*, defined as epilepsy, or by epileptiform activity, the equivalent activity pattern, *in vitro*. Thus epileptic activity represents both an inducing insult and the main characteristic of epilepsy. The pathophysiological mechanisms leading from the induction to the expression of spontaneous recurrent seizures are still not clear; the classical view implicates an imbalance between excitation and inhibition. In attempts to identify factors causing such an imbalance, past studies have mainly focused on functional alterations in inhibition as well as on morphological changes such as neuronal cell loss (excitatory and inhibitory) and mossy fibre sprouting (for review see Sutula *et al.* 1988; Dalby & Mody, 2001). Yet little is known about whether and how epileptic activity changes excitatory synaptic transmission. This information, however, is essential to understand how epilepsy is generated and how it affects a neural network. We experimentally addressed this issue by determining the effects of epileptiform activity on excitatory synaptic transmission in area CA1 of the hippocampus. For this purpose we treated cultured hippocampal slices overnight with the specific $GABA_A$ receptor antagonist (–)-bicuculline methochloride (BMC, 50 μM).

Methods

Hippocampal slice cultures

Organotypic hippocampal slice cultures were prepared from 6-day-old Wistar rat pups killed by decapitation (Gähwiler *et al.* 1997), following a protocol approved by the Veterinary Department of the Canton of Zurich. After 2 weeks *in vitro*, slices were randomly allocated into three groups that were incubated for 15 ± 3 h (overnight) either in serum-based medium alone or in medium containing BMC (50 μM), or BMC plus the specific NMDA receptor antagonist (R,E)-4-(3-phosphonoprop-2-enyl)piperazine-2-carboxylic acid (CPP 40 μM; donated by Novartis, Basel, Switzerland).

Electrophysiology

Field recordings of spontaneous bursting activity were performed at 35°C (incubation temperature) with patch pipettes (3–5 MΩ) containing 2 M NaCl in culture medium. Whole-cell voltage-clamp recordings of excitatory synaptic currents were obtained using an Axopatch 200B amplifier (Axon Instruments, Foster City,

 DOI: 10.1113/jphysiol.2003.052662

CA, USA) and pipettes containing (mM): 140 potassium or caesium gluconate, 10 KCl, 5 Hepes, 1.1 EGTA, 4 $MgCl_2$, 10 phosphocreatine, pH 7.3, 285 mosmol l^{-1}, unless otherwise stated. Slices were perfused with warmed (32°C) saline containing (mM): 137 NaCl, 2.7 KCl, 2.8 $CaCl_2$ 2 $MgCl_2$, 11.6 $NaHCO_3$, 0.4 NaH_2PO_4, 5.6 glucose and phenol red (10 mg l^{-1}), pH 7.4, unless otherwise mentioned. Only cells with a series resistance between 10 and 15 MΩ were included.

Miniature excitatory postsynaptic currents (mEPSCs) were recorded at –70 mV in the presence of 0.5 μM tetrodotoxin (TTX, Latoxan, Valence, France), 50 μM picrotoxin, 50 μM BMC and 40 μM CPP using potassium gluconate-based intracellular solution (see above). Miniature inhibitory postsynaptic currents (mIPSCs) were recorded at –70 mV in the presence of 0.5 μM TTX, 20 μM 2,3-dioxo-6-nitro-1,2,3,4-tetrahydrobenzo(f)quinoxaline-7-sulphonamide (NBQX) and 40 μM CPP using the following intracellular solution (mM): 140 caesium gluconate, 10 NaCl, 1 MgCl, 10 Hepes, 0.4 Mg_2GTP, 0.1 EGTA, pH 7.3, 285 mosmol l^{-1}. mEPSCs and mIPSCs were analysed offline with the 'Mini Analysis Program' (Synaptosoft, Leonia, CA, USA) using a detection threshold of 5 pA. Cumulative histograms were constructed by pooling 300 consecutive events from each cell. Average traces were obtained for each experiment by aligning individual mEPSCs to their rising phases; fitting a single exponential on the 90–10% of the decaying signal yielded the decay time constant.

Excitatory postsynaptic currents (EPSCs) were evoked using a monopolar glass stimulation electrode filled with extracellular medium and placed into stratum radiatum close to the recording electrode, in the presence of 50 μM picrotoxin, 50 μM BMC, 4 mM Mg^{2+} and 4 mM Ca^{2+}, and after a cut between CA3 and CA1. AMPA receptor-mediated EPSCs were evoked at –70 mV, whereas NMDA receptor-mediated EPSCs were evoked at +40 mV during blockade of AMPA receptors by application of 20 μM NBQX.

Field excitatory postsynaptic potentials (fEPSPs) were recorded in the stratum radiatum of the CA1 region with a glass electrode containing 2 M NaCl and 3 mM BMC after cutting between areas CA3 and CA1. Stimuli (0.1 ms) were delivered to CA3 axons at 0.25 Hz by a bipolar glass electrode filled with extracellular solution. LTP was induced by theta burst stimulation composed of five trains at 5 Hz, each consisting of five stimuli delivered at 100 Hz. LTD was induced by stimulating at 3 Hz for 5 min (Dudek & Bear, 1992). The levels of potentiation and depression were estimated for each cell by measuring the average slope of field potentials in the middle third of its rising phase over 5 min taken 25 min after the end of LTP or LTD induction and were expressed as a percentage of baseline slope.

Average values are expressed as means ± S.E.M. Statistical comparisons were made using the Student's *t* tests. Drugs were from either Tocris Cookson (Bristol, UK) or Sigma (Buchs, Switzerland), unless otherwise specified.

Preparation and application of Semliki Forest virus vectors

The cDNA for green fluorescent protein (GFP)-tagged GluR1 (Mack *et al.* 2001) was inserted into the *Xho*I and *Avr*II sites of the pSFV2gen vector, yielding pSFV2gen-GFP-GluR1. Viral particles were produced according to our standardized procedure (Ehrengruber, 2002). Slices were injected with diluted (1 : 50) virus stock over two or three sites in the CA1 pyramidal cell layer, returned to the incubator, and cultured for an additional 2 days.

Confocal microscopy and image analysis

Optical stacks (27.2 μm × 27.2 μm, step size 0.5 μm, 8-bit, 512 × 512 pixels) were acquired on a Leica SP2 confocal microscope (Leica Microsystems, Heidelberg, Germany) equipped with a heated (32°C) perfusion chamber and a HCX APO × 63 water immersion objective lens (NA = 0.9). No averaging was employed, laser power, gain and offset of the photomultipliers were equal for corresponding images. Spines were identified in images obtained in control and BMC containing medium. Relative spine fluorescence was determined by averaging pixel values usually over two layers containing spines and also from the equivalent places before treatment. Mean values of spine fluorescence measured after overnight incubation (after) were normalized to mean values before incubation (before) both in control and BMC-treated slices. Background fluorescence in nearby regions without any obvious structures was subtracted from all measurements. Images shown are maximal intensity projections of several optical sections, median filtered with pixel width 1. All analysis was performed with ImageJ (National Institutes of Health, USA).

Results

Disinhibition-induced epileptiform activity is epileptogenic

Recordings of field potentials in the CA1 stratum radiatum under culture conditions (perfusion of culture medium at 35°C) revealed that acute application of BMC induced

epileptiform bursts (burst frequency: 0.05 ± 0.007 Hz, burst duration: 4.2 ± 0.6 s, $n = 17$, Fig. 1*A*) that were never observed in control conditions ($n = 17$, Fig. 1*B*) and correspond to synchronous population activity of neurones within the culture (Traub & Wong, 1982).

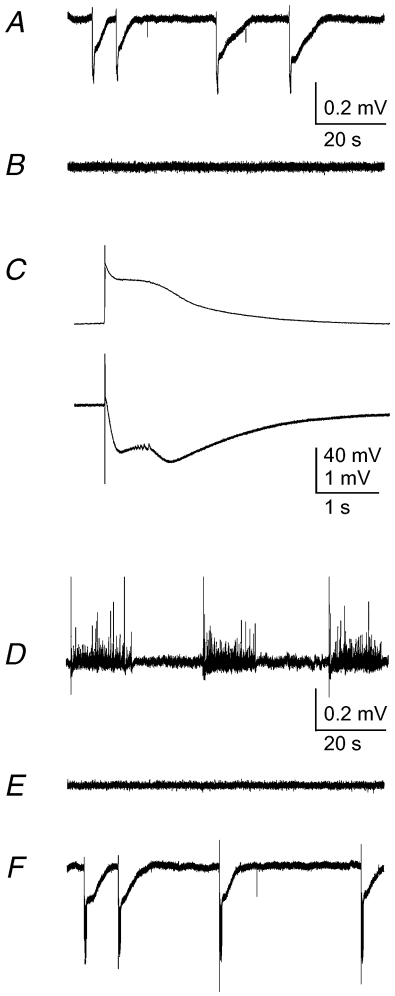

Figure 1. Epileptiform activity has an NMDA receptor-dependent epileptogenic effect
A, B, D–F, sample traces of field potential recordings in the stratum radiatum of hippocampal CA1 region. *A,* acute application of the $GABA_A$ receptor antagonist BMC induced population bursts, which appear in field recordings as large current sinks. *B,* under control conditions stable baseline field recordings were observed. *C,* simultaneous intracellular recording of the membrane potential of a CA1 pyramidal cell (upper trace) and field recording from the CA3 stratum radiatum (lower trace) during a population burst, showing that the postsynaptic cell is depolarized during presynaptic activity. *D* and *E,* epileptiform activity was still present after washout of overnight-applied BMC *(D)*, but stopped after washout of overnight-applied BMC + CPP *(E)*. *F,* blockade of both $GABA_A$ and NMDA receptors by acute application of BMC and CPP, respectively, did not prevent bursting activity.

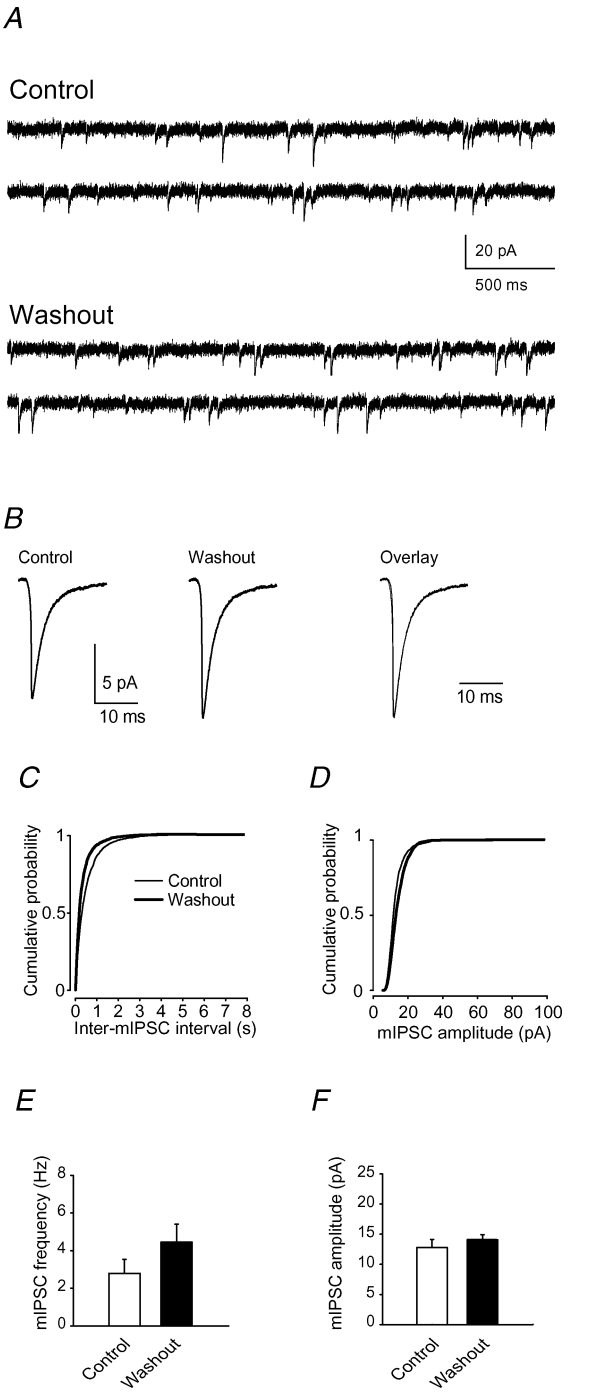

Figure 2. Synaptic inhibition is restored after washout of overnight-applied BMC
A, sample traces of mIPSCs recorded from CA1 pyramidal cells in control conditions and after washout of BMC. *B*, averaged traces of mIPSCs from control slices and after washout of BMC. Scaled and superimposed traces of averaged mIPSCs show no change in kinetics in the two conditions. *C* and *D*, cumulative distributions of mIPSC interevent intervals (*C*) and amplitudes (*D*) are not significantly different. *E* and *F*, summary plots showing no significant change in the frequency (*E*) and the amplitude (*F*) of mIPSCs in control slices and after washout of overnight-applied BMC.

Epileptiform bursts lasted longer than 500 ms and were thus classified as ictal activity (see Karnup & Stelzer, 2001). Simultaneous recordings of field potentials in the CA3 region (presynaptic activity) and the membrane potential of a CA1 pyramidal cell (postsynaptic activity) revealed that during bursting pre- and postsynaptic cells are activated concomitantly ($n = 3$, Fig. 1*C*). Bursting was still present after overnight incubation in BMC-containing medium, suggesting that slices have an ability to burst during the entire period of disinhibition ($n = 13$); in addition, burst frequency was significantly higher after overnight incubation than after acute BMC application (burst frequency: 0.13 ± 0.032 Hz, $n = 13$, $P = 0.02$), suggesting that prolonged disinhibition accelerates bursting.

Next, we studied the epileptogenic effect of bursting activity, i.e. whether prolonged bursting activity promotes spontaneous epileptiform activity after recovery of inhibition. The majority of slices (7 of 9) exhibited spontaneous epileptiform activity after overnight BMC incubation and its subsequent washout, achieved by changing the culture medium 5 times in 5 h (Fig. 1*D*). Washout of BMC resulted in bursting activity different from that observed in the presence of the drug (compare Fig. 1*A* and *D*), most probably because of restored inhibition. In five slices ictal activity was observed, whereas two slices exhibited interictal activity (burst duration < 500 ms; see Karnup & Stelzer, 2001). Burst duration and frequency (ictal and interictal activity), were 5.4 ± 2.5 s and 0.3 ± 0.1 Hz ($n = 7$), respectively. To exclude the possibility that the observed busting activity arises from incomplete washout of BMC, we compared mIPSCs recorded from CA1 pyramidal cells in control conditions and after washout of the drug. We found no significant change in the amplitude (control: 12.78 ± 1.35 pA, $n = 6$, washout of BMC: 14.08 ± 0.84 pA, $n = 6$, $P = 0.43$, Fig. 2) and the frequency (control: 2.79 ± 0.74 Hz, washout of BMC: 4.4 ± 0.9 Hz, $P = 0.2$, Fig. 2) of mIPSCs in the two conditions. These results indicate that inhibition is fully recovered after washout of BMC, and therefore

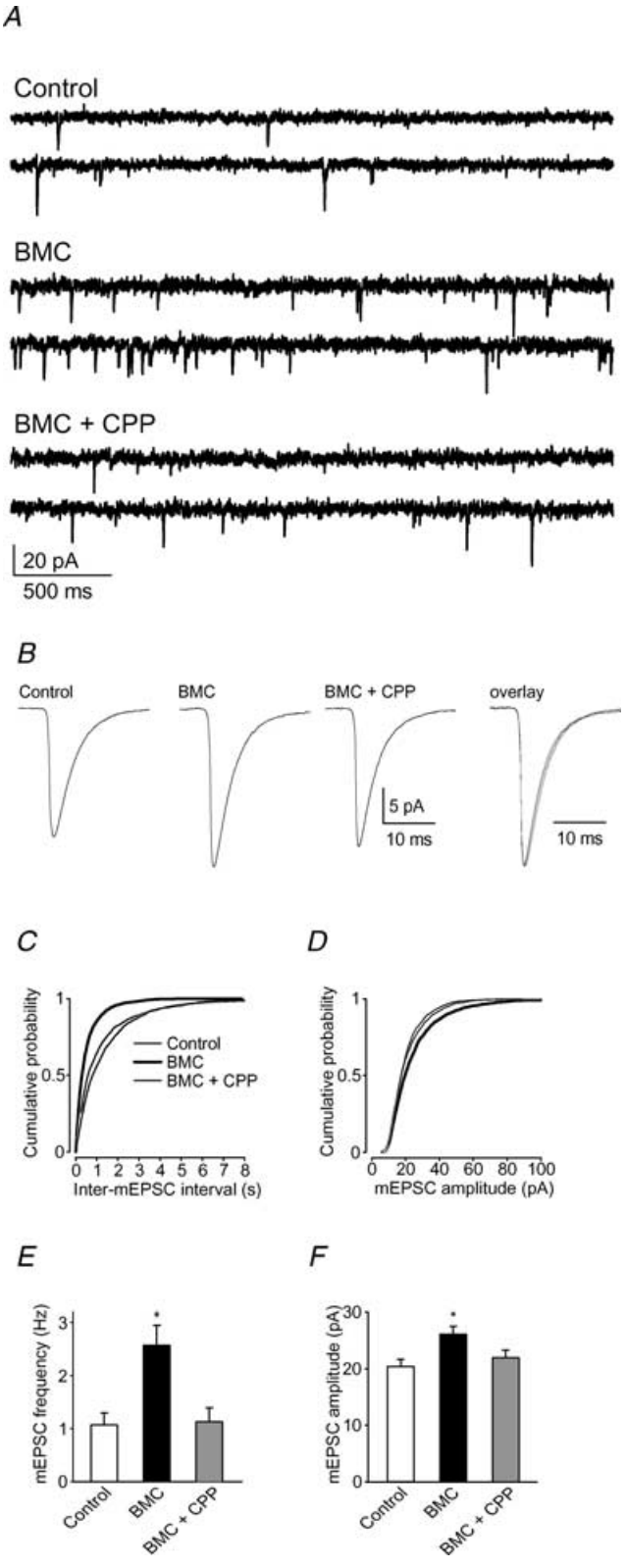

Figure 3. Epileptiform activity leads to an NMDA receptor-dependent increase in the frequency and amplitude of AMPA receptor-mediated mEPSCs

A, sample traces of mEPSCs recorded from CA1 pyramidal cells in control, BMC- and BMC + CPP-treated slices. *B,* averaged traces of mEPSCs from control, BMC− and BMC + CPP-treated slices. Scaled and superimposed traces of averaged mEPSCs show no change in kinetics in the three conditions. *C* and *D*, cumulative distributions of mEPSC interevent intervals and amplitudes showing a shift toward shorter interevent intervals *(C)* and higher amplitudes *(D)* in BMC-treated slices. Blockade of NMDA receptors prevented both shifts (BMC + CPP). *E* and *F,* summary graphs showing a significantly higher mEPSC frequency *(E)* and amplitude *(F)* in BMC-treated slices compared to control and BMC + CPP-treated slices. Asterisks indicate statistical significance ($P < 0.05$).

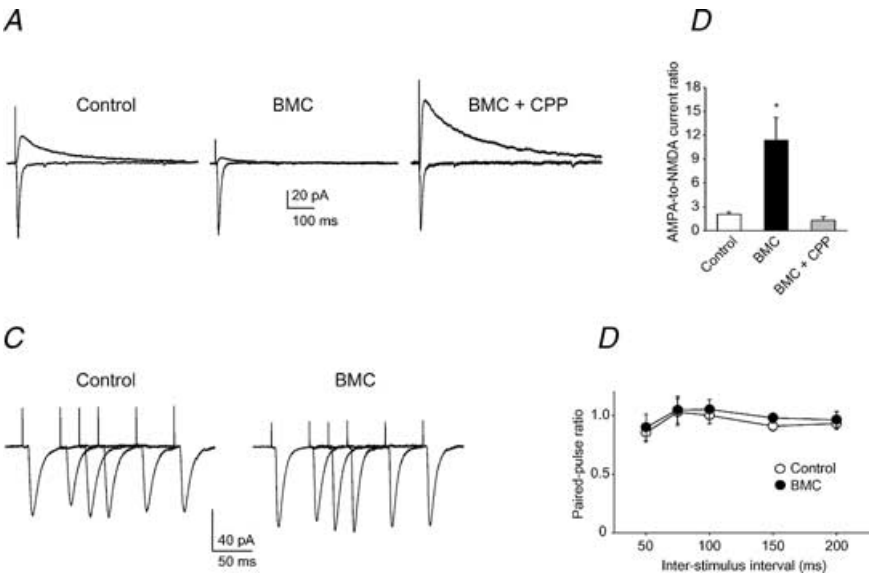

Figure 4. Bursting increases the AMPA-to-NMDA current ratio in an NMDA receptor-dependent manner, but fails to affect paired-pulse ratio of AMPA receptor-mediated EPSCs

A, superimposed averaged traces of evoked AMPA and NMDA receptor-mediated EPSCs recorded in the same cell at –70 mV (lower traces) and +40 mV (upper traces), respectively, in control, BMC− and BMC + CPP-treated slices. *B,* summary graph showing a significant increase of AMPA-to-NMDA current ratio after overnight bursting (BMC) compared to control and BMC + CPP-treated slices. Asterisk indicates statistical significance ($P < 0.05$). *C*, superimposed averaged traces of AMPA receptor-mediated EPSCs evoked by paired-pulse stimulation at different time intervals recorded from a cell in control and in a BMC-treated slice. *D,* summary plot of paired-pulse ratios of AMPA receptor-mediated EPSCs showing no significant difference in control and BMC-treated slices.

spontaneous epileptiform activity cannot be explained by a reduction in inhibitory synaptic transmission.

To test whether this epileptogenic effect of bursting is NMDA receptor dependent, we incubated slices overnight in BMC and the NMDA receptor antagonist (CPP, 40 μM) (BMC + CPP), and recorded field potentials after washout of both drugs. NMDA receptor blockade prevented spontaneous epileptiform activity in 5 of 7 slices (Fig. 1*E*), indicating that NMDA receptor-dependent changes in the network underlie the epileptogenic effect of bursting. To rule out the possibility that NMDA receptor blockade prevented bursting itself, thereby inhibiting its epileptogenic effect, we assessed the effect of acute CPP application on BMC-induced bursting. Blockade of NMDA receptors did not change burst frequency (BMC + CPP: 113 ± 17% of BMC alone, $P = 0.47$ paired t test, $n = 7$, Fig. 1*F*) and duration (BMC + CPP: 110 ± 9% of BMC alone, $P = 0.29$ paired t test), but decreased the area under the burst (BMC + CPP: 69 ± 7% of BMC alone, $P = 0.01$ paired t test), indicating that NMDA receptors are activated during bursting but are neither necessary for burst initiation nor termination. Taken together, these results suggest that bursting activity has an epileptogenic effect which is mediated via NMDA receptor activation.

Epileptiform activity enhances AMPA receptor-mediated synaptic transmission

To examine whether epileptiform activity affects excitatory synaptic transmission, we recorded AMPA receptor-mediated mEPSCs from CA1 pyramidal cells that had burst overnight. We found a significant increase in both the frequency (control: 1.06 ± 0.2 Hz, $n = 10$, BMC: 2.56 ± 0.3 Hz, $n = 7$, 241 ± 28% of control, $P = 0.002$, Fig. 3) and the amplitude (control: 20.4 ± 1.2 pA, $n = 10$; BMC: 26 ± 1.3 pA, $n = 7$, 127 ± 6.3% of control, $P = 0.021$, Fig. 3) of mEPSCs in BMC-treated slices. No changes in the 10–90% rise time (control: 1.15 ± 0.05 ms, $n = 10$, BMC: 1.15 ± 0.13 ms, $n = 7$, 100 ± 11% of control, $P = 0.99$), the decay time constant (control: 3.78 ± 0.11 ms; BMC: 3.46 ± 0.41 ms, 92 ± 10% of control, $P = 0.4$), the input resistance (control: 138 ± 6 MΩ, BMC: 143 ± 7 MΩ, 104 ± 5% of control, $P = 0.57$) and the membrane capacitance (control: 110 ± 8 pF, BMC: 104 ± 5 pF, 95 ± 5% of control, $P = 0.61$) were found after overnight bursting. The increase in mEPSC frequency may be due to a higher probability of vesicular glutamate release or alternatively to an increased number of functional synapses. To test the first possibility, we measured the amplitude ratio of evoked AMPA receptor-mediated EPSCs in response to

paired-pulse stimulation of CA3 axons at different time intervals (50, 75, 100, 150 and 200 ms). A change in this ratio reflects a change in the probability of vesicular release (Debanne *et al.* 1996). There were no significant differences in the paired-pulse ratios of evoked AMPA receptor-mediated EPSCs at any of the intervals tested between control and BMC-treated slices ($P > 0.26$ at all intervals, $n = 5$ in each group, Figs 4*C* and *D*), suggesting no change in the probability of vesicular release.

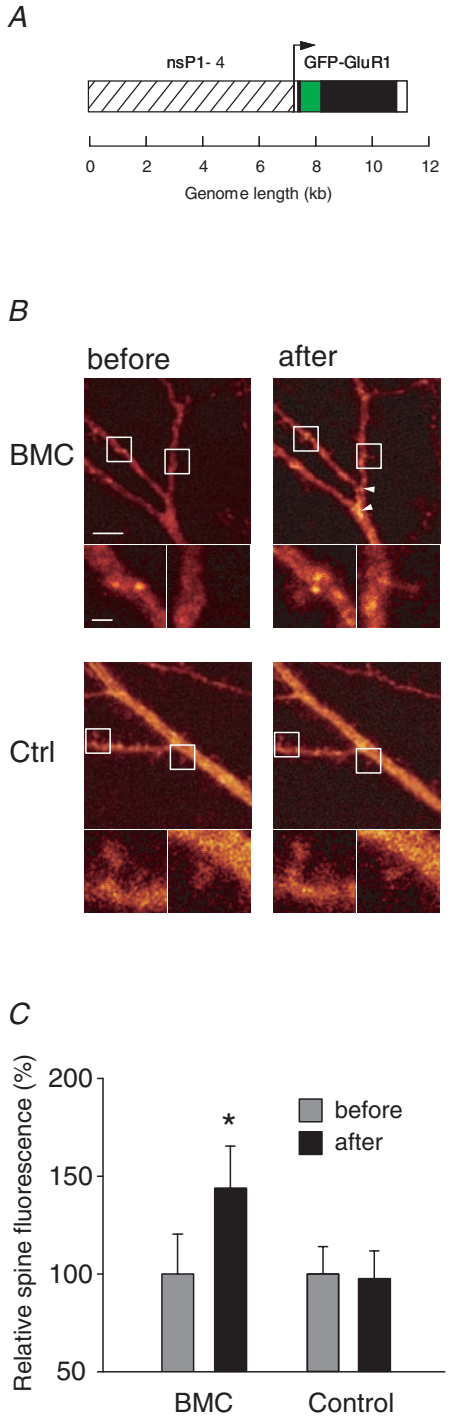

The bursting-induced increase in the frequency of mEPSCs may also arise from the conversion of silent into functional synapses, where silent synapses display only NMDA receptor-mediated EPSCs (Isaac *et al.* 1995; Liao *et al.* 1995; Durand *et al.* 1996), and functional synapses display both AMPA and NMDA receptor-mediated EPSCs. We investigated this possibility by measuring the ratio between the amplitudes of the AMPA and NMDA receptor-mediated components of synaptic currents evoked at –70 mV and +40 mV, respectively. We found a significantly higher AMPA-to-NMDA current ratio in BMC-treated slices compared to control (control: 2.0 ± 0.27, $n = 8$, BMC: 11.3 ± 2.8, $n = 11$, 565 ± 140% of control, $P = 0.014$, Fig. 4*A* and *B*), suggesting that overnight bursting converts silent into functional synapses.

Next, we tested whether the enhancement of synaptic transmission shows NMDA receptor dependence, by incubating slices overnight in medium containing BMC + CPP. Although this treatment did not have a major effect on BMC-induced bursting (see Fig. 1*F*), it prevented the rise in mEPSC frequency (1.12 ± 0.27 Hz, $n = 8$, 105.6 ± 25.4% of control, $P = 0.86$, Fig. 3) and amplitude (21.4 ± 1.3 pA, $n = 8$, 104.9 ± 6.3% of control, $P = 0.41$, Fig. 3), as well as the increase of the AMPA-to-NMDA current ratio (1.3 ± 0.4, $n = 5$, 65 ± 20% of control, $P = 0.15$, Fig. 4*A* and *B*), without affecting the kinetics of mEPSCs (10–90% rise time: BMC + CPP: 1.03 ± 0.06 ms, $n = 8$, 90 ± 5% of control, $P = 0.2$; decay time constant: BMC + CPP: 3.63 ± 0.20 ms, 95 ± 5% of control, $P = 0.5$). Taken together, these data show that epileptiform activity

Figure 5. Bursting activity induces delivery of GluR1-GFP to spines

A, schematic representation of the viral vector used herein. SFV-GFP-GluR1 encodes non-structural proteins nsP1-4 (hatched) driving the expression of GluR1 (black) with a GFP tag near the 5′-end (green) (GluR1-GFP). White areas depict the multiple cloning site and the 3′-non-translated region; the arrow indicates the start of the subgenomic RNA containing the transgene. *B,* maximal intensity projection of confocal sections showing apical dendritic segments of a CA1 pyramidal cell from a BMC-treated slice (top), obtained shortly before incubation in BMC (before) and 12 h later (after). Images from a control slice were taken at the corresponding time points (bottom) (scale bar, 5 μm). For each panel, two regions of interest are selected (squares) and shown at higher magnification below the panel (scale bar, 1 μm). BMC incubation revealed more putative spines due to fluorescence appearance whereas fluorescence in putative spines in control conditions did not significantly change. Bursting also induced the formation of fluorescence clusters in dendrites (arrowheads), which were not observed in control slices. *C,* summary plot showing a significant increase in spine fluorescence after overnight bursting and no change in control slices. Asterisk indicates statistical significance ($P < 0.05$).

leads to an NMDA receptor-dependent activation of silent synapses and to potentiation of functional synapses.

Epileptiform activity promotes delivery of GluR1-GFP to dendritic spines

To directly monitor the redistribution of AMPA receptors following epileptiform activity, we overexpressed recombinant green fluorescent protein-tagged GluR1 AMPA receptor subunits (GluR1-GFP) (Mack *et al.* 2001) in CA1 pyramidal cells using a Semliki Forest virus expression system (Ehrengruber, 2002) (Fig. 5*A*). These recombinant subunits can form homomeric receptors that are translocated into synapses upon tetanic stimulation but that remain largely excluded from synapses under normal synaptic transmission (Shi *et al.* 2001). Two days post transfection, we collected confocal images of GFP fluorescence from primary and secondary apical dendrites before and after overnight incubation with BMC. Bursting led to a significant increase in fluorescence in dendritic spines (143 ± 21.6% of before, $P = 0.0002$ paired t test, $n = 26$ spines in $n = 5$ slices, Figs 5*B* and *C*), whereas the amount of fluorescence at the corresponding location in images obtained before bursting was often near the background level. The mean spine fluorescence did not change in control slices (97 ± 14% of before, $P = 0.62$ paired t test, $n = 15$ spines in $n = 8$ slices, Figs 5*B* and *C*). Often we found that bursting activity induced formation of fluorescence clusters in dendrites, which we did not further quantify. Given that most excitatory synapses of CA1 pyramidal cells are localized on dendritic spines, the translocation of GluR1-GFP into spines suggests that bursting activity drives AMPA receptors into synapses.

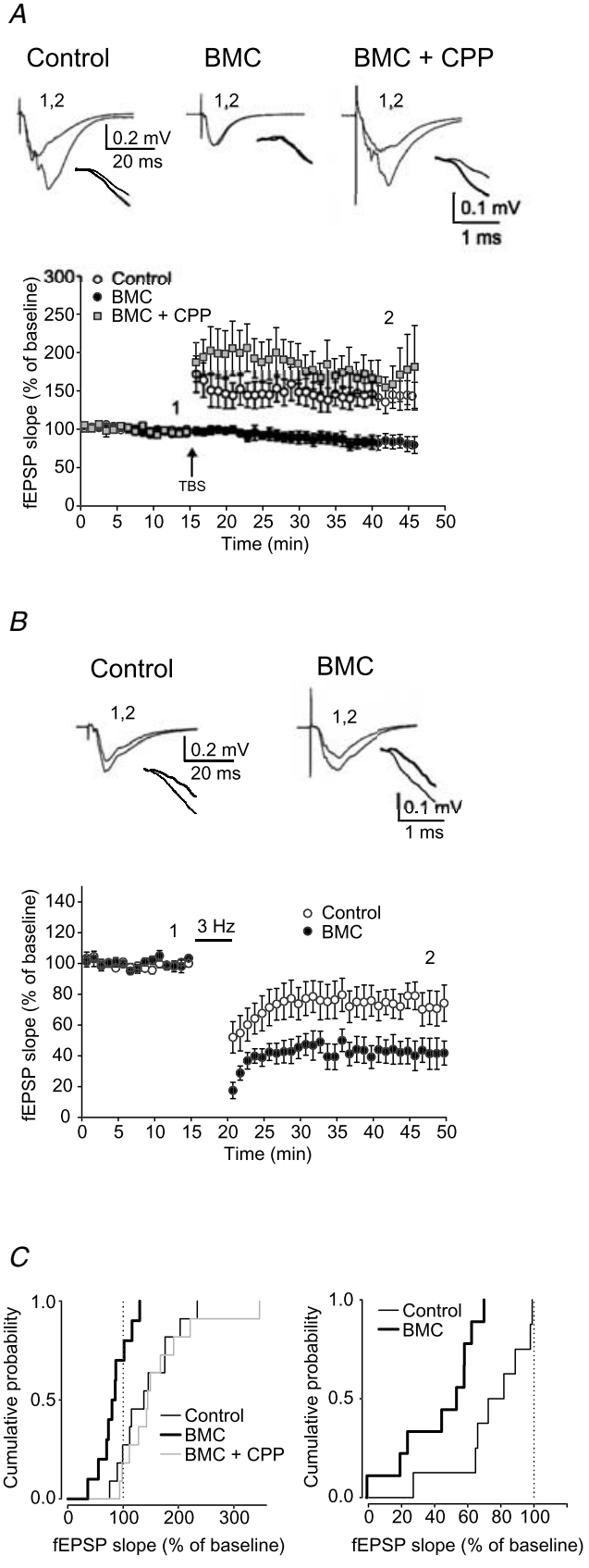

Figure 6. CA3–CA1 synapses express no LTP and increased LTD after overnight epileptiform activity

A, summary graph showing that theta burst stimulation (TBS) induced stable LTP in both control slices and slices that had been exposed to BMC + CPP for overnight, whereas no potentiation could be elicited in BMC-treated slices. Each symbol represents the normalized slope of fEPSPs averaged during 1 minute. Superimposed averaged traces of field potentials evoked at labelled time points are illustrated above the graph. Insets show the superimposed rising phases of fEPSPs on an expanded time scale. *B,* summary graph showing that 3 Hz stimulation induced significantly higher LTD in BMC-treated slices than in controls. Superimposed averaged traces of field potentials evoked at marked time points are shown above the graph. Insets show superimposed rising phases of fEPSPs on an expanded time scale. *C,* cumulative distribution plots of changes in baseline fEPSP slope after induction of LTP (left) and LTD (right) in control, BMC−, and BMC + CPP-treated slices show level of plasticity for individual experiments.

Epileptiform activity occludes LTP and enhances LTD

An NMDA receptor-dependent increase in synaptic transmission, as we observe after bursting, is known to occur during LTP in area CA1 (Collingridge *et al.* 1983). Moreover, Hebbian conditions for LTP induction are established during bursting, i.e. pre- and postsynaptic cells are activated simultaneously (see Fig. 1*C*). It is therefore conceivable that bursting-induced synaptic strengthening and LTP share the same expression mechanism. If this is the case, then LTP induced with a conventional stimulation protocol should be reduced or even occluded after overnight bursting. To test this possibility, we compared the degree of potentiation in control, BMC- and BMC + CPP-treated slices after theta burst stimulation of CA3 axons. Stable LTP lasting at least 30 min was induced in control slices (142 ± 15% of baseline fEPSP slope, $n = 11$, $P = 0.011$, Fig. 6*A* and *C*) whereas no LTP could be elicited in BMC-treated slices (83 ± 9% of baseline fEPSP slope, $n = 10$, $P = 0.08$, Fig. 6*A* and *C*). When NMDA receptors were blocked during overnight epileptiform activity, thereby preventing synaptic strengthening, LTP of similar magnitude as in control slices was induced after washout of CPP (163 ± 22% of baseline fEPSP slope, $n = 11$, $P = 0.01$, Fig. 6*A* and *C*). These results show that synapses that were strengthened by overnight bursting cannot be further potentiated, indicating that epileptiform activity and LTP have a common expression mechanism.

If bursting-induced synaptic potentiation represents LTP, then subsequently induced LTD should be enhanced (Rioult-Pedotti *et al.* 2000). To test this, we compared the amount of LTD induced by low frequency stimulation of CA3 axons in BMC-treated slices and control slices. As expected, we found a significantly higher LTD in slices that had shown bursting activity overnight (44 ± 8% of baseline fEPSP slope, $n = 9$, $P < 0.01$ relative to baseline, $P = 0.014$ relative to control after depression, Figs 6*B* and *C*) compared to control slices (76 ± 8% of baseline fEPSP slope, $n = 8$, $P = 0.01$, Figs 6*B* and *C*).

The occlusion of LTP and the enhancement of LTD are consistent with the hypothesis that the bursting-induced strengthening of CA3–CA1 synapses corresponds to LTP.

Discussion

Our data indicate that epileptiform activity leads to an NMDA receptor-dependent enhancement of AMPA receptor-mediated transmission of CA3–CA1 synapses, thereby preventing additional synaptic potentiation and increasing synaptic depression.

Epileptiform activity caused a significant increase in the frequency and amplitude of AMPA receptor-mediated mEPSCs. mEPSC frequency varies with the number of functional synapses on a given cell and with the probability of vesicular release, whereas the number and/or conductance of receptors within a synapse define the amplitude. Prolonged bursting could increase mEPSC frequency by increasing the probability of vesicular release. However, our data are not consistent with this hypothesis as the presynaptic parameter paired-pulse ratio was unchanged after overnight bursting, and the increase in mEPSC frequency was blocked by NMDA receptor antagonists despite a maintained high level of neuronal activity. Our data suggest, rather, that bursting-induced activation of silent synapses accounted for the increase in mEPSC frequency. In support of this, we observed an increase in the evoked AMPA-to-NMDA current ratio after bursting. This ratio represents the relative AMPA and NMDA receptor content at both functional and silent synapses. The more than 5-fold increase in the AMPA-to-NMDA current ratio was accompanied by a 30% increase in mEPSC amplitude, suggesting that potentiation of functional synapses only partially accounted for the observed increase in the AMPA-to-NMDA current ratio and implying a major contribution from silent synapse activation. Taken together, these results show that bursting increases the number of functional AMPA receptors in both functional and silent synapses. Alternatively, a decrease in NMDA receptor-mediated synaptic transmission may contribute to a bursting-induced increase in AMPA-to-NMDA current ratio. Although we did not directly investigate NMDA receptor function, the changes in mEPSCs, GluR1-GFP trafficking, and LTP/LTD levels clearly identify AMPA receptor-mediated synaptic transmission as a target of epileptiform activity. Moreover, the ability to induce LTD, which is NMDA receptor-dependent at the CA3–CA1 synapse (Debanne *et al.* 1994), indicates that NMDA receptors remain functional after bursting.

That bursting enhances excitatory synaptic transmission is supported by our finding that disinhibition led to spine delivery of GluR1-GFP. In line with this, it has been recently shown that LTP induction relocalizes alphavirally overexpressed recombinant GluR1 to the synapse (Hayashi *et al.* 2000). Hence, we presume that bursting also leads to the insertion of GluR1-GFP in synapses which are localized on dendritic spines. As reported by Shi *et al.*, we also observed dendritic clusters of GluR1-GFP after epileptiform activity, the meaning of which is obscure and has been suggested to be related to the spine apparatus (Shi *et al.* 1999).

After overnight epileptiform activity, no LTP could be induced with theta burst stimulation, indicating that synapses were already maximally potentiated, i.e. bursting raised the level of baseline synaptic efficacy to its maximal state. Since the amounts of bi-directional plastic changes depend on the level of baseline synaptic efficacy (Rioult-Pedotti *et al.* 2000; Savic *et al.* 2003), it was not surprising that occlusion of LTP was accompanied by a concomitant increase of LTD in slices that had shown bursting activity overnight. Thus bursting and tetanic stimulation both activate the same pathway resulting in potentiation of excitatory synapses. This view is additionally supported by our finding that bursting, like LTP, increases synaptic efficacy through activation of NMDA receptors (see Figs 1, 3 and 6).

The strengthening of excitatory synapses during bursting potentially affects all excitatory synapses that have the capacity for NMDA receptor-dependent plasticity. This strengthening will reinforce the excitatory network and may shift the balance of excitation and inhibition towards excitation, thereby increasing the bursting probability (Bains *et al.* 1999; Staley *et al.* 2001). We suggest that bursting-induced reinforcement of the excitatory network accounts for the sustained spontaneous bursting that we observed after BMC washout. In line with this, when synaptic strengthening was prevented by NMDA receptor blockade during bursting, no spontaneous epileptiform activity was observed after washout of BMC and CPP. We speculate that reinforcement of the excitatory network represents a final common pathway on to which all epilepsy models that use high neuronal activity as an induction stimulus converge. This shift may also explain how seizure foci can spread from one brain region to another, as occurs during secondary epileptogenesis (Mayersdorf & Schmidt, 1982).

Several factors including changes in inhibitory synaptic transmission, alterations in membrane transporters and synaptic reorganization may participate in the induction and maintenance of seizure activity. Our data are not consistent with a change in inhibition (see Fig. 2), but rather emphasize the role of strengthening excitatory synaptic connections through an LTP-like mechanism, as postulated previously (Ben-Ari & Represa, 1990). Our findings are consistent with results from kindled rats which display progressively increasing EPSPs in the course of kindling (Sutula & Steward, 1986) and with reports showing that bursting activity potentiates excitatory synapses (Buzsaki *et al.* 1987; Schneiderman *et al.* 1994; Bains *et al.* 1999) and that NMDA receptor antagonists can prevent (Ben-Ari & Gho, 1988; Croucher *et al.* 1988; Stasheff *et al.* 1989) or delay epileptogenesis (Sato *et al.* 1988; Durmuller *et al.* 1994; DeLorenzo *et al.* 1998).

As LTP is thought to be involved in memory acquisition (see, e.g. Tsien *et al.* 1996), bursting-induced LTP occlusion may explain the transient decrease in learning ability observed after seizures (Cain *et al.* 1993; McNamara *et al.* 1993; Rutten *et al.* 2002). Accordingly, we speculate that the recovery of memory formation after cessation of seizure activity (Cain *et al.* 1993; Rutten *et al.* 2002) mirrors the time course of LTP decay (Villarreal *et al.* 2002).

References

Bains JS, Longacher JM & Staley KJ (1999). Reciprocal interactions between CA3 network activity and strength of recurrent collateral synapses. *Nat Neurosci* **2**, 720–726.

Ben-Ari Y & Gho M (1988). Long-lasting modification of the synaptic properties of rat CA3 hippocampal neurones induced by kainic acid. *J Physiol* **404**, 365–384.

Ben-Ari Y & Represa A (1990). Brief seizure episodes induce long-term potentiation and mossy fibre sprouting in the hippocampus. *Trends Neurosci* **13**, 312–318.

Buzsaki G, Haas HL & Anderson EG (1987). Long-term potentiation induced by physiologically relevant stimulus patterns. *Brain Res* **435**, 331–333.

Cain DP, Hargreaves EL, Boon F & Dennison Z (1993). An examination of the relations between hippocampal long-term potentiation, kindling, afterdischarge, and place learning in the water maze. *Hippocampus* **3**, 153–163.

Collingridge GL, Kehl SJ & McLennan H (1983). Excitatory amino acids in synaptic transmission in the Schaffer collateral-commissural pathway of the rat hippocampus. *J Physiol* **334**, 33–46.

Commission on Classification and Terminology of the International League Against Epilepsy. (1989). Proposal for revised classification of epilepsies and epileptic syndromes. *Epilepsia* **30**, 389–399.

Croucher MJ, Bradford HF, Sunter DC & Watkins JC (1988). Inhibition of the development of electrical kindling of the prepyriform cortex by daily focal injections of excitatory amino acid antagonists. *Eur J Pharmacol* **152**, 29–38.

Dalby NO & Mody I (2001). The process of epileptogenesis: a pathophysiological approach. *Curr Opin Neurol* **14**, 187–192.

Debanne D, Gähwiler BH & Thompson SM (1994). Asynchronous pre- and postsynaptic activity induces associative long-term depression in area CA1 of the rat hippocampus in vitro. *Proc Natl Acad Sci U S A* **91**, 1148–1152.

Debanne D, Guerineau NC, Gähwiler BH & Thompson SM (1996). Paired-pulse facilitation and depression at unitary synapses in rat hippocampus: quantal fluctuation affects subsequent release. *J Physiol* **491**, 163–176.

DeLorenzo RJ, Pal S & Sombati S (1998). Prolonged activation of the N-methyl-D-aspartate receptor-Ca2+ transduction pathway causes spontaneous recurrent epileptiform discharges in hippocampal neurons in culture. *Proc Natl Acad Sci U S A* **95**, 14482–14487.

Dudek SM & Bear MF (1992). Homosynaptic long-term depression in area CA1 of hippocampus and effects of N-methyl-D-aspartate receptor blockade. *Proc Natl Acad Sci U S A* **89**, 4363–4367.

Durand GM, Kovalchuk Y & Konnerth A (1996). Long-term potentiation and functional synapse induction in developing hippocampus. *Nature* **381**, 71–75.

Durmuller N, Craggs M & Meldrum BS (1994). The effect of the non-NMDA receptor antagonist GYKI 52466 and NBQX and the competitive NMDA receptor antagonist D-CPPene on the development of amygdala kindling and on amygdala-kindled seizures. *Epilepsy Res* **17**, 167–174.

Ehrengruber MU (2002). Alphaviral vectors for gene transfer into neurons. *Mol Neurobiol* **26**, 183–201.

Gähwiler BH, Capogna M, Debanne D, McKinney RA & Thompson SM (1997). Organotypic slice cultures: a technique has come of age. *Trends Neurosci* **20**, 471–477.

Goddard GV (1967). Development of epileptic seizures through brain stimulation at low intensity. *Nature* **214**, 1020–1021.

Hayashi Y, Shi SH, Esteban JA, Piccini A, Poncer JC & Malinow R (2000). Driving AMPA receptors into synapses by LTP and CaMKII: requirement for GluR1 and PDZ domain interaction. *Science* **287**, 2262–2267.

Isaac JT, Nicoll RA & Malenka RC (1995). Evidence for silent synapses: implications for the expression of LTP. *Neuron* **15**, 427–434.

Karnup S & Stelzer A (2001). Seizure-like activity in the disinhibited CA1 minislice of adult guinea-pigs. *J Physiol* **532**, 713–730.

Liao D, Hessler NA & Malinow R (1995). Activation of postsynaptically silent synapses during pairing-induced LTP in CA1 region of hippocampal slice. *Nature* **375**, 400–404.

Mack V, Burnashev N, Kaiser KM, Rozov A, Jensen V, Hvalby O, Seeburg PH, Sakmann B & Sprengel R (2001). Conditional restoration of hippocampal synaptic potentiation in Glur-A-deficient mice. *Science* **292**, 2501–2504.

McNamara RK, Kirkby RD, dePape GE, Skelton RW & Corcoran ME (1993). Differential effects of kindling and kindled seizures on place learning in the Morris water maze. *Hippocampus* **3**, 149–152.

Mayersdorf A & Schmidt RPE (1982). Secondary Epileptogenesis. Raven Press, New York.

Rioult-Pedotti MS, Friedman D & Donoghue JP (2000). Learning-induced LTP in neocortex. *Science* **290**, 533–536.

Rutten A, van Albada M, Silveira DC, Cha BH, Liu X, Hu YN, Cilio MR & Holmes GL (2002). Memory impairment following status epilepticus in immature rats: time-course and environmental effects. *Eur J Neurosci* **16**, 501–513.

Sato K, Morimoto K & Okamoto M (1988). Anticonvulsant action of a non-competitive antagonist of NMDA receptors (MK-801) in the kindling model of epilepsy. *Brain Res* **463**, 12–20.

Savic N, Lüthi A, Gähwiler BH & McKinney RA (2003). N-methyl-D-aspartate receptor blockade during development lowers long-term potentiation threshold without affecting dynamic range of CA3-CA1 synapses. *Proc Natl Acad Sci U S A* **100**, 5503–5508.

Schneiderman JH, Sterling CA & Luo R (1994). Hippocampal plasticity following epileptiform bursting produced by GABAA antagonists. *Neuroscience* **59**, 259–273.

Shi S, Hayashi Y, Esteban JA & Malinow R (2001). Subunit-specific rules governing AMPA receptor trafficking to synapses in hippocampal pyramidal neurons. *Cell* **105**, 331–343.

Shi SH, Hayashi Y, Petralia RS, Zaman SH, Wenthold RJ, Svoboda K & Malinow R (1999). Rapid spine delivery and redistribution of AMPA receptors after synaptic NMDA receptor activation. *Science* **284**, 1811–1816.

Staley KJ, Bains JS, Yee A, Hellier J & Longacher JM (2001). Statistical model relating CA3 burst probability to recovery from burst-induced depression at recurrent collateral synapses. *J Neurophysiol* **86**, 2736–2747.

Stasheff SF, Anderson WW, Clark S & Wilson WA (1989). NMDA antagonists differentiate epileptogenesis from seizure expression in an in vitro model. *Science* **245**, 648–651.

Sutula T, He XX, Cavazos J & Scott G (1988). Synaptic reorganization in the hippocampus induced by abnormal functional activity. *Science* **239**, 1147–1150.

Sutula T & Steward O (1986). Quantitative analysis of synaptic potentiation during kindling of the perforant path. *J Neurophysiol* **56**, 732–746.

Traub RD, Miles R & Jefferys JG (1993). Synaptic and intrinsic conductances shape picrotoxin-induced synchronized after-discharges in the guinea-pig hippocampal slice. *J Physiol* **461**, 525–547.

Traub RD & Wong RK (1982). Cellular mechanism of neuronal synchronization in epilepsy. *Science* **216**, 745–747.

Tsien JZ, Huerta PT & Tonegawa S (1996). The essential role of hippocampal CA1 NMDA receptor-dependent synaptic plasticity in spatial memory. *Cell* **87**, 1327–1338.

Villarreal DM, Do V, Haddad E & Derrick BE (2002). NMDA receptor antagonists sustain LTP and spatial memory: active processes mediate LTP decay. *Nat Neurosci* **5**, 48–52.

Acknowledgements

We thank M. Scanziani for fruitful discussions and suggestions, Volker Mack for subcloning GluR1-GFP into pSFV2gen, K. Lundstrom for help with the SFV technology, C. Gee and S. Hugel for reading the manuscript, and H. Kasper and L. Rietschin for technical assistance. This work was supported by the Swiss National Science Foundation (31-61518.00) and the NCCR on Neural Plasticity and Repair.